Dielectric Relaxation of Cationic Surfactants in Aqueous Solution. 2. Solute Relaxation

Christian Baar, Richard Buchner,* and Werner Kunz

Institut für Physikalische und Theoretische Chemie, Universität Regensburg, D-93040 Regensburg, Germany

Received: December 11, 2000

The complex dielectric permittivity spectra of octyl-, dodecyl-, and hexadecyltrimethylammonium bromide and of dodecyltrimethylammonium chloride reveal two low-frequency relaxation processes centered around 80 and 250 MHz. These are assigned to the diffusional relaxation of free and bound counterions, respectively, around the charged micelles. It is found that at low concencentrations the model of Grosse is able to rationalize simultaneously the amplitudes and relaxation times of both relaxation processes. The similar model of Pauly and Schwan, which is restricted to the relaxation of the bound counterions, fits the parameters of the 250 MHz process over the entire concentration range. Both models were used to determine the radius and surface conductivity of the micelles. Volume fractions determined from these radii are in good agreement with literature data and with values obtained from the analysis of the water relaxation processes. This shows that the complex permittivity spectra of theses solutions, determined in the range $0.09 \leq \nu/\mathrm{GHz} \leq 89$, can be assigned to microscopic processes in a consistent way. Additionally, the data suggest that for octyltrimethylammonium bromide solutions below the critical micelle concentration, cmc, the 250 MHz relaxation is due to the tumbling motion of solvent-separated ion pairs formed with an association constant of $K_A \approx 26$. This mechanism contributes also significantly above the cmc. The surprising presence of the 80 MHz relaxation process also at submicellar concentrations of C_8TAB may hint for a premicellar aggregation of surfactant ions.

1. Introduction

Understanding the physicochemical properties of self-assembling systems of amphiphilic molecules in aqueous solution is relevant for many fields of pure and applied science.[1] Especially, micellar aggregates of surfactants have attracted considerable interest over the past decades, not only because of their technical importance but also due to their role as models for several biochemical and pharmacological systems.[2] Nevertheless, our knowledge is far from complete and especially for the dielectric properties systematic studies are scarce and the interpretation of the results is ambiguous.

To rationalize the dielectric behavior of charged colloidal systems, including micelles, various theories have been proposed. These predict either a single-step[3−5] or a two-step relaxation mechanism[6−8] with or without a continuous distribution of relaxation times. However, it seems that a rigorous test of these theories was hampered by insufficient data. Previous DRS investigations into micellar solutions of alkyltrimethylammonium salts showed that in addition to the water relaxation region in the gigahertz range there is at least one dispersion step around a few hundred megahertz which can be attributed to the solute. Commonly, this relaxation mode is described by a Cole−Cole relaxation-time distribution and assigned to the polarization of the counterion distribution around the charged micelle.[3,9,10] Discussed mechanisms were the deformation of the diffuse counterion cloud, that is the well-known Debye−Falkenhagen effect,[11] or a tangential current in the layer of bound counterions moving with the micelle, Figure 1. Only recently were Shikata and Imai able to resolve two relaxation processes due to micelles.[12] Following the arguments of previous studies, the authors assigned the low-frequency dispersion step, $\Delta\epsilon_s$, of their spectra, centered around 30 MHz (relaxation time $\tau_s \approx 5$ ns), to the polarization of the diffuse counterion cloud around the micelle. For the high-frequency process of amplitude $\Delta\epsilon_f$, peaking in the 300 MHz region ($\tau_f \approx 0.5$ ns), the rotation of alkyltrimethylammonium bromide ion pairs on the surface of the micelles was postulated as a novel mechanism. However, these findings may be disputed in view of the assumptions Shikata and Imai had to make on the water relaxation due to their small frequency range of $0.002 \leq \nu/\mathrm{GHz} \leq 2$. Thus, a major aim of the present contribution, which complements a previous paper on the water relaxation in alkyltrimethylammonium halide solutions, is to seek a consistent interpretation of micelle and solvent relaxation modes in surfactant solutions deduced from complex permittivity spectra covering $0.09 \leq$

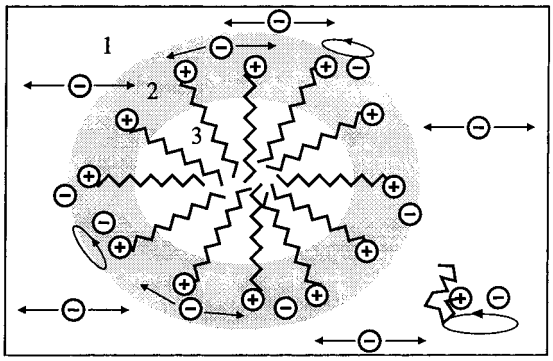

Figure 1. Schematic view of a micelle: (1) the region of the diffuse cloud of mobile counterions and ion pairs; (2) polar surface layer formed by charged headgroups of the surfactant cations and bound anions; (3) nonpolar, hydrophobic core. According to Part 1, micelle hydration is characterized by Z_{ib} bound H_2O molecules per headgroup in region (2) and Z_s "slow" H_2O molecules interacting with a hydrophobic tail in the boundary of the regions (2) and (3).[17]

* Corresponding author. E-mail: Richard.BBuchner@chemie.uni-regensburg.de.

10.1021/jp004450p CCC: $20.00
Published on Web 03/23/2001

TABLE 1: Eyring Activation Enthalpies, $\Delta H^{\ddagger}$, and Entropies, $\Delta S^{\ddagger}$, of the Solute Relaxation Times τ_1 and τ_2 at the Surfactant Molalities m[a]

system	τ_i	$\Delta H^{\ddagger}$	$\Delta S^{\ddagger}$
C_8TAB	τ_1	-1.4 ± 6.6	-85 ± 22
$m = 0.10292$	τ_2	11.6 ± 1.3	-21 ± 5
C_{12}TAB	τ_1	-5.8 ± 5.8	-97 ± 19
$m = 0.33017$	τ_2	13.8 ± 0.8	-17 ± 3
C_{16}TAB	τ_1	14.0 ± 4.9	-33 ± 16
$m = 0.33802$	τ_2	18.6 ± 2.0	-4 ± 6
C_{12}TAC	τ_1	1.3 ± 3.6	-71 ± 12
$m = 0.32950$	τ_2	17.0 ± 1.3	-5 ± 5

[a] Units: m in mol/kg, $\Delta H^{\ddagger}$ in kJ/mol, and $\Delta S^{\ddagger}$ in J/(mol K). The covered temperature range is $28 \le \vartheta/°C \le 65$ for C_{16}TAB and $0 \le \vartheta/°C \le 65$ elsewhere.

υ/GHz $\le$ 89. As will be shown, the splitting of the micelle relaxation into two dispersion steps proposed by ref 12 is indeed correct. However, due to repercussions from the water relaxation region their parameters appear to be systematically shifted.

2. Results

In a previous publication,[17] quoted as part 1 furtheron, complex dielectric permittivity spectra, $\hat{\epsilon}(\upsilon)$, of aqueous solutions of octyl- (C_8TAB), dodecyl- (C_{12}TAB), and hexadecyltrimethylammonium bromide (C_{16}TAB) and of dodecyltrimethylammonium chloride (C_{12}TAC) were presented, which cover the concentration range $0.1 \le c/\text{mol dm}^{-3} \le 1$. It was shown that in the investigated frequency range, $0.09 \le \upsilon/\text{GHz} \le 89$, the dielectric relaxation behavior can be generally represented by a superposition of five Debye relaxation processes. The dispersion steps with the relaxation times $\tau_3 \approx 25$ ps, $\tau_4 \approx 8$ ps, and $\tau_5 \approx 1$ ps were assigned to "slow" H_2O molecules, bulk water, and "mobile" H_2O, respectively. The amplitudes S_i, $i = 3 \ldots 5$, of these processes were discussed in terms of micelle hydration.

In addition to the solvent relaxation two dispersion steps, with $\tau_1 \approx 1.5$ ns and $\tau_2 \approx 300$ ps, could be resolved in the low-frequency region of $\hat{\epsilon}(\upsilon)$. Their limiting permittivities, ϵ_i, $i = 1, \ldots, 3$, defining the dispersion amplitudes (relaxation strengths) $S_1 = \epsilon_1 - \epsilon_2$ and $S_2 = \epsilon_2 - \epsilon_3$, and the corresponding relaxation times, τ_1 and τ_2, are summarized in Tables S1−S7 of the Supporting Information accompanying part 1. Representative examples of the data are given in Figures 4, 6, and 7 of this contribution. Although the slow process is situated at the edge of the experimentally accessible frequency range, leading to a considerable scatter of S_1 and τ_1, it could be detected for all investigated surfactants over the entire concentration range. τ_1 is rather independent of the surfactant concentration, c, but increases with the length of the alkyl chain. Except for C_{16}TAB, $\Delta H^{\ddagger}(\tau_1) \approx 0$ is found for the Eyring enthalpies of activation, whereas for the corresponding entropy $\Delta S^{\ddagger}(\tau_1) < 0$ is obtained; see Table 1. This rather strange temperature dependence is possibly the consequence of insufficient frequency coverage and thus will not be discussed further. After a rapid increase, the amplitude S_1 seems to level at intermediate concentrations. τ_2 increases from C_8TAB to C_{16}TAB and also from chloride to bromide but decreases with c except for C_8TAB. The enthalpy of activation is in the range $12 \le \Delta H^{\ddagger}(\tau_2)/(\text{kJ/mol}) \le 19$ (see Table 1), increasing with increasing chain length of the surfactant and when going from Br^- to Cl^-. $\Delta S^{\ddagger}(\tau_2)$ is negative and increases in the same sequence. For C_8TAB S_2 increases monotonically, whereas for longer chain lengths a pronounced maximum is observed. Surprisingly, for C_8TAB two relaxation processes are also observed at $c <$ cmc. For this region only the relaxation of ion pairs in the bulk solution is expected; see Figure 1.

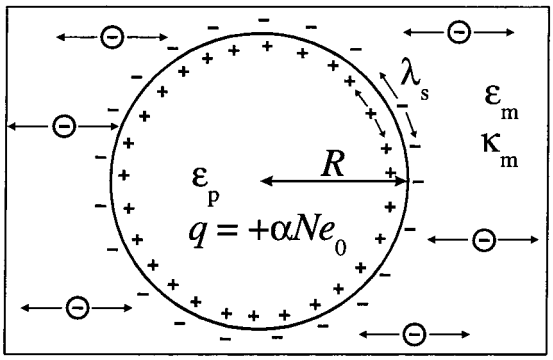

Figure 2. Schematic representation of Grosse's model for polyions in solution: The spherical polyion of charge q, radius R, core permittivity ϵ_p and surface conductance λ_s is immersed in a medium of permittivity ϵ_m and conductivity κ_m.[8]

At low concentrations a comparison with the relaxation parameters of ref 12 is possible for C_{12}TAB and C_{16}TAB. Taking into account the significant noise in both studies, $S_1 \approx \Delta\epsilon_s$ and $\tau_2 \approx \tau_f$. Additionally, a similar trend of the relaxation times with chain length is observed. However, S_2 is significantly smaller than $\Delta\epsilon_f$ and also $\tau_1 < \tau_s$. A likely reason for the difference in amplitudes is the smaller frequency range, which forced Shikata and Imai to assumptions regarding the water contribution to $\hat{\epsilon}(\upsilon)$. On the other hand, the value obtained for the relaxation time of the slow process is very sensitive to the choice of the conductivity correction applied to extract the dielectric loss, $\epsilon''(\upsilon)$, from the experimentally accessible total loss; see part 1. It is interesting to note that for the solution of 0.1 mol dm^{-3} C_{12}TAB, which was investigated by Barchini and Pottel[3] and our laboratory in the same frequency range, the same permittivity contribution of bulk water was found although the relaxation models applied for data analysis differ considerably. This suggests that the rather broad Cole−Cole distribution used in ref 3 to fit the micelle relaxation region covers $S_1 + S_2 + S_3$ of the present investigation, i.e., includes the dispersion step of slow water.

3. Discussion

Dodecyl- and Hexadecyltrimethylammonium Halide Surfactants. Because cmc < 0.025 mol dm^{-3} the solute contribution to the dielectric properties of C_{12}TAC, C_{12}TAB, and C_{16}TAB solutions can be reasonably attributed to micelles alone. The relaxation of possible ion pairs formed by monomeric surfactant cations and Br^- or Cl^-, which was observed for C_8TAB with cmc = 0.284 mol dm^{-3} (see below) would be too small to be detected. Thus, the relaxation parameters S_1, τ_1, S_2, and τ_2, can be directly used to test available models for the relaxation of the charge distribution around (spherical) micelles. The theories of O'Konski,[4] Schwarz,[5] and Barchini and Pottel,[3] predicting a single dispersion step, as well as the models of Pauly and Schwan,[6] Schurr,[7] and Grosse,[8] yielding two dispersion steps, were considered.

It turns out that only the approaches of Pauly and Schwan and of Grosse, which are similar in some respect, yield a reasonable description of (at least parts of) the experimental data. Both models consider a spherical particle of radius R, dielectric permittivity ϵ_p, and conductivity κ_p suspended in a medium of dielectric permittivity ϵ_m and conductivity κ_m. In Grosse's model for a micelle (see Figure 2) the sphere is isolating, $\kappa_p = 0$, but bears a charge $q = \alpha N e_0$.[8] N is the

aggregation number of the micelle, ϵ_0 the elementary charge, and α the degree of counterion dissociation. This core is surrounded by an infinitely thin conducting surface of surface conductivity λ_s, arising from the tangential motion of $(1-\alpha)N$ associated (bound) counterions. The dissociated fraction of the counterions forms a diffuse ion cloud that is characterized by the Debye length

$$\chi^{-1} = \sqrt{\frac{\epsilon_0 \epsilon_m D}{\kappa_m}} \tag{1}$$

χ^{-1} depends on the diffusion coefficient, D, of the ions; ϵ_0 is the permittivity of the vacuum. Note that in our study no co-ions are present. Thus, the electroneutrality condition requires that at equilibrium *all* halide ions present in the solution are either bound to (adsorbed at) some micelle or belong to its diffuse ion cloud.[13−15] Due to their high mobility compared to the charged micelles, essentially the anions in the diffuse ion clouds determine κ_m. For convenience we will designate these as "free anions" furtheron. The term "bound" will be restricted to the cations adsorbed at (associated with) the micelles.

Grosse was able to show that for such a model of a micelle solution two dispersion steps occur. Provided the volume fraction of the micelles, p, is small and $R \gg \chi^{-1}$ analytical expressions can be given for the relaxation parameters.[8] The low-frequency relaxation mode is characterized by the mean relaxation time

$$\tau_{G1} \approx \frac{R^2}{D} \tag{2}$$

and the dispersion amplitude

$$S_{G1} = \frac{9p\epsilon_m (2\chi\lambda_s/\kappa_m)^4}{16\left[\frac{2\chi\lambda_s}{\kappa_m}\left(\frac{2\lambda_s}{R\kappa_m}+1\right)+2\right]^2} \tag{3}$$

This ion-cloud relaxation reflects the radial diffusion of the ions in the solution surrounding the suspended particle.

The high-frequency dispersion step with

$$\tau_{G2} = \frac{\epsilon_0 \epsilon_m \left(\frac{\epsilon_p}{\epsilon_m}+2\right)}{\kappa_m \left(\frac{2\lambda_s}{R\kappa_m}+2\right)} \tag{4}$$

and

$$S_{G2} = \frac{9p\epsilon_m \left(\frac{2\lambda_s}{R\kappa_m}-\frac{\epsilon_p}{\epsilon_m}\right)^2}{\left(\frac{\epsilon_p}{\epsilon_m}+2\right)\left(\frac{2\lambda_s}{R\kappa_m}+2\right)^2} \tag{5}$$

is assigned to the rapid tangential motion of bound counterions on the surface of the micelles. Grosse was able to show that for $2\lambda_s/(R\kappa_m) \gg \epsilon_p/\epsilon_m$ these expressions reduce to the result for the Maxwell−Wagner relaxation of a suspension of insulating particles covered by a conducting layer.

The theory dealing with the Maxwell−Wagner effect due to the interfacial polarization of a heterogeneous dielectric was given by Pauly and Schwan.[6] The authors consider an uncharged sphere, surrounded by a shell of thickness d, permittivity ϵ_s, and conductivity κ_s (see Figure 3). The shell is identified with

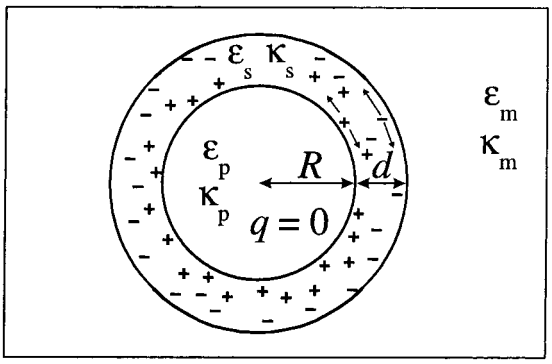

Figure 3. Schematic representation of the model of Pauly and Schwan: The uncharged spherical particle of core radius R, core permittivity ϵ_p, and core (volume) conductivity κ_p, surrounded by a surface layer of thickness d, permittivity ϵ_s, and (volume) conductivity κ_s, is immersed in a medium of permittivity ϵ_m and conductivity κ_m.[6]

the outer region of the micelle, containing some hydrocarbon, the charged headgroups, hydration water, and the Stern layer formed by the associated (bound) counterions. As a consequence, the fluctuation of the surrounding ion cloud is beyond the scope of this theory. On the other hand, the model is more general with respect to the properties of the sphere itself, and in its general form, the model is not restricted to low volume fractions p of the particles. Because of the presence of three phases two dispersion steps are obtained, irrespective of the choice of the conductivities κ_p, κ_s, and κ_m and of the permittivities ϵ_p, ϵ_s, and ϵ_m. The amplitudes are given by the equations

$$S_{P1} = \frac{\epsilon_0\epsilon_m - \kappa_m\tau_1}{\epsilon_0 C(\tau_2-\tau_1)\tau_1}[-A\tau_1^2 + E\tau_1 - B] \tag{6}$$

$$S_{P2} = \frac{\epsilon_0\epsilon_m - \kappa_m\tau_2}{\epsilon_0 C(\tau_2-\tau_1)\tau_2}[A\tau_2^2 - E\tau_2 + B] \tag{7}$$

For the relaxation times

$$\tau_{P1} = \frac{F}{2C}\left[1 - \sqrt{1-\frac{4DC}{F^2}}\right] \tag{8}$$

$$\tau_{P2} = \frac{F}{2C}\left[1 + \sqrt{1-\frac{4DC}{F^2}}\right] \tag{9}$$

is obtained. The abbreviations in eqs 6−9 are

$$A = (1+2p)\kappa_s a + 2(1-p)\kappa_m b$$

$$B = (1+2p)\epsilon_0^2\epsilon_s c + 2(1-p)\epsilon_0^2\epsilon_m d_1$$

$$C = (1-p)\kappa_s a + (2+p)\kappa_m b$$

$$D = (1-p)\epsilon_0^2\epsilon_s c + (2+p)\epsilon_0^2\epsilon_m d_1$$

$$E = (1+2p)[\epsilon_0\epsilon_s a + \epsilon_0\kappa_s c] + 2(1-p)[\epsilon_0\epsilon_m b + \epsilon_0\kappa_m d_1]$$

$$F = (1-p)[\epsilon_0\epsilon_s a + \epsilon_0\kappa_s c] + (2+p)[\epsilon_0\epsilon_m b + \epsilon_0\kappa_m d_1]$$

$$a = (1+2v)\kappa_p + 2(1-v)\kappa_s$$

$$b = (1-v)\kappa_p + (2+v)\kappa_s$$

$$c = (1+2v)\epsilon_p + 2(1-v)\epsilon_s$$

$$d_1 = (1-v)\epsilon_p + (2+v)\epsilon_s$$

$$v = \left(\frac{R}{R+d}\right)^3$$

TABLE 2: Parameters of Grosse's Model for Alkyltrimethylammonium Halide Solutions at Room Temperature and Fractions (1 − α) of Bound Counterions from the Literature[a]

surfactant	C_8TAB	C_{12}TAB	C_{16}TAB	C_{12}TAC
ϵ_m[b]	78.34	78.34	77.28	78.34
ϵ_p	2	2	2	2
N	20[c]	47[d]	104[d]	32[d]
D_-[e]	2.080	2.080	2.080	2.032
fit 1: R fixed, λ_s variable				
R	1.76[f]	2.28[d]	2.80[d]	2.13[d]
λ_s[g]	1.92	2.30	3.10	2.45
fit 2: R and λ_s variable				
R[g]	1.66	2.17	2.40	1.96
λ_s[g]	2.28	2.43	3.49	2.66
1 − α	0.65[c]	0.77[h]	0.83[h]	0.58[h]

[a] Units: R in 10^{-9} m, D_- in 10^{-9} m^2/s, λ_s in 10^{-9} Ω^{-1}. [b] Reference 20. [c] Reference 18. [d] Radius of the equivalent sphere calculated from ref 19. [e] Reference 21. [f] Estimated from refs 18 and 19. [g] Fit parameter. [h] Reference 22.

p is the volume fraction of the entity particle plus shell, of radius $R_m = R + d$. Formally, both processes can be described by Debye equations. Both models yield the radius of the micelle, R_m, which allows us to calculate the corresponding volume fraction as

$$p = \frac{4}{3}\pi R_m^3 N_A \frac{c - \mathrm{cmc}}{N} \qquad (10)$$

In eq 10 c is the molar concentration of the solution and N is the aggregation number. The concentration of free monomers is given by $c_{mon} = \mathrm{cmc}$.[16] For Grosse's model $R_m = R$ and for the model of Pauly and Schwan $R_m = R + d$.

Table 2 summarizes the concentration-independent input data for the application of Grosse's model to the investigated systems and the obtained results. As the permittivity of the medium, ϵ_m, the value of pure water at 25 °C (C_{16}TAB: 28 °C) is taken. This is a reasonable approximation due to the low concentration of free surfactant ions and the weak interactions of the halide ions with the solvent; see part 1. For the conductivity of the medium, κ_m, the experimental conductivity of the solutions is inserted (tabulated in the Supporting Information of part 1). In eqs 1 and 2 the diffusion coefficient, D_-, of the appropriate halide ion in bulk water is inserted, as the cation contribution is negligible. For the dielectric constant of the micelles, $\epsilon_p = 2$, a value typical for pure hydrocarbons, is taken. This is probably too low as the considered sphere, in addition to the hydrophobic tails, also includes (part of) the headgroups and even some water molecules, as discussed in part 1. However, test calculations revealed that ϵ_p can be varied over a wide range without significantly changing the results of the analysis. For the aggregation number, N, and the radius, R, of the micelles, data determined by small-angle neutron scattering (SANS)[18,19] were inserted. For ellipsoidal micelles R is the radius of the equivalent sphere with the same volume. A necessary adjustable parameter of Grosse's model is the unknown surface conductivity λ_s. The radius R of the micelles is either taken from literature, fit 1 of Table 2, or also varied as a fit parameter (fit 2). The relaxation times τ_1 and τ_2 as well as the dispersion amplitudes S_1 and S_2 were fitted simultaneously. As the model was derived for low volume fractions of the particles, the data are weighted by $1/c$.

Table 2 summarizes the results of the one- and two-parameter fits for all examined surfactants. As can be seen from Figure 4 for C_{12}TAB, Grosse's model is well suited to describe the concentration dependence of amplitudes and relaxation times

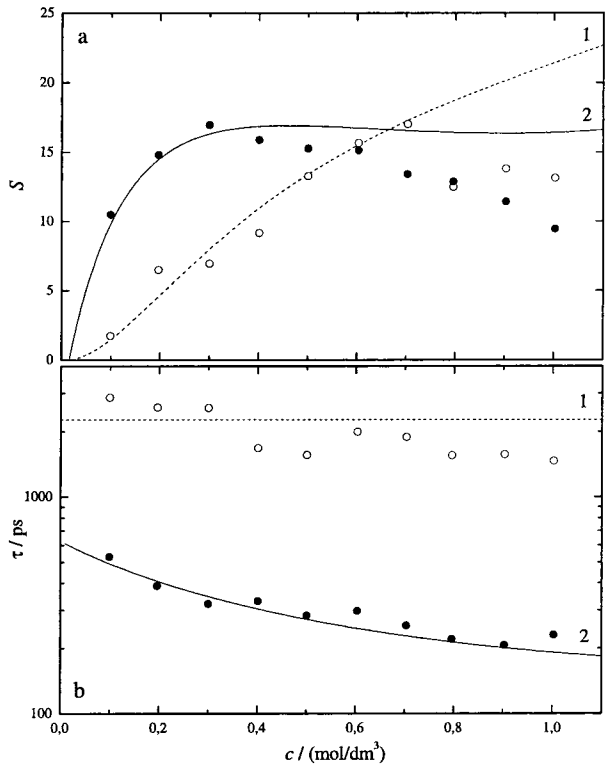

Figure 4. (a) Experimental dispersion amplitudes, S_i, and (b) relaxation times, τ_i, of the micelle relaxation processes $i = 1$ (○) and $i = 2$ (●) of C_{12}TAB at 25 °C. The lines give the fits of Grosse's model for $i = 1$ (broken) and $i = 2$ (solid).

of both micelle relaxation processes up to $c \approx 0.4$ mol/dm^3. Similar fits were obtained for C_{12}TAC and C_{16}TAB. As expected from the limitations of the theory, the fit curves for the amplitudes, S_1 and S_2, deviate considerably at higher concentrations. However, the relaxation times, especially τ_2, which reflects the mobility of the bound counterions on the surface of the micelles, are well fitted over the entire concentration range. Immediate conclusion from the applicability of Grosse's theory at low concentrations is that the experimentally observed low-frequency dispersion step (S_1, τ_1) can be assigned to the fluctuations of the diffuse ion cloud surrounding the micelles. This corroborates Shikata and Imai's interpretation of their τ_s based on eq 2 only.[12] S_2 and τ_2 reflect the amount and the mobility of the bound counterions. The values obtained for R with the two-parameter fit compare well with the SANS results of ref 19, but are generally smaller by about 5−10%. The larger deviation for C_{16}TAB definitely arises from too small values of τ_1, but for the other surfactants this is probably not the case. Figure 5 shows that the volume fraction of the micelles calculated from R with eq 10 agree remarkably well with p obtained from the analysis of the solvent relaxation processes in a completely different approach; see part 1. Larger deviations between both methods are only found for C_{16}TAB, where p determined from the water dispersion steps is more reliable. Figure 5 implies that the water molecules hydrating the micelles reside within the sphere determined by Grosse's R. Note that the good agreement of the volume fractions determined from the micelle relaxation processes and from the water dispersion steps strongly supports the used superposition of five Debye equations for fitting $\hat{\epsilon}(\nu)$. It is very unlikely that a band-fitting model—essentially preferred for numerical reasons—is able to yield consistent results for a quantity like p without touching the essential physics of the investigated system.

The second information obtained from fitting Grosse's model

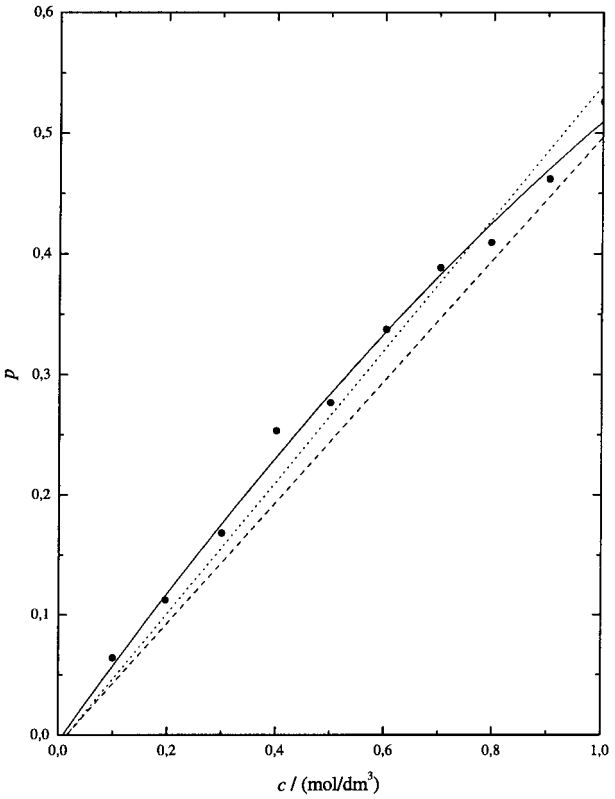

Figure 5. Volume fraction p of $C_{12}TAB$ micelles determined from the amount of free water (●, solid line) and with eq 10 from the radii determined with the models of Grosse (dotted line) and of Pauly and Schwan (broken line).

is the surface conductivity λ_s, lines 7 and 9 of Table 2, which is a measure for the amount *and* the mobility of the counterions bound to the surface of the micelle. For the common counterion Br^- λ_s increases with increasing R, parallel to the fraction of bound counterions, $1 - \alpha$ (last line of Table 2). When going from Br^- to Cl^- λ_s also increases. Since $1 - \alpha$ decreases it seems that here the different mobilities of the anions are reflected. It would be interesting to relate these results to lateral surface diffusion coefficients that can be obtained with NMR spectroscopy. However, to our knowledge only $C_{16}TAB$ was examined until now.[23] Note that neither the theory of Grosse nor that of Pauly and Schwan discussed below specify how $\lambda_s > 0$ and $\kappa_s > 0$, respectively, arise. Hopping of the bound halide ions between different surfactant headgroups is a possible mechanism, but so is the rotation of ion pairs discussed by Shikata and Imai.[12]

By definition Grosse's model is unsuitable for high micelle concentrations. This should not be the case for the model of Pauly and Schwan, eqs 6−9. On the other hand, the fluctuation of the diffuse ion cloud, which can be definitely assigned to the experimentally observed low-frequency process (S_1, τ_1) on the basis of Grosse's model, is beyond the scope of the theory proposed by Pauly and Schwan. As it turns out, the parameters S_{P1} and τ_{P1} of their model can be identified with the experimental data S_2 and τ_2. The second dispersion step of the model (S_{P2}, τ_{P2}) is also of the Maxwell−Wagner type and important, e.g., for cell suspensions. However, for micelles with an isolating sphere surrounded by a conducting shell, the predicted magnitude $S_{P2} \leq 0.02$ is well below the noise level of our experiment. Thus, the application of eqs 6−9 is not inconsistent with the simultaneous use of Grosse's model.

Table 3 summarizes the input quantities used for the fit and the obtained parameters. The inner sphere of Figure 3 is assumed

TABLE 3: Parameters of the Model of Pauly and Schwan for Alkyltrimethylammonium Halide Solutions at Room Temperature and Derived Surface-Layer Diffusion Coefficients, $D^S(X^-)$, of Bound Anions[a]

surfactant	C_8TAB	$C_{12}TAB$	$C_{16}TAB$	$C_{12}TAC$
ϵ_m[b]	78.34	78.34	77.28	78.34
ϵ_s	38[c]	33[d]	28[d]	32[d]
ϵ_p	2	2	2	2
κ_p	0	0	0	0
N	20[e]	47[f]	104[f]	32[f]
R	0.7[g]	1.38[h]	2.10[h]	1.23[h]
fit parameters				
κ_s	5.7	6.0	6.5	7.7
d	0.76	0.73	0.62	0.67
d [f]		0.9	0.7	0.9
$D^S(X^-)$	0.82	0.75	0.55	1.39

[a] Units: κ_p, κ_s in S/m, R and d in 10^{-9} m, $D^S(X^-)$ in 10^{-9} m^2 s^{-1}. [b] Reference 20. [c] Estimated from ref 24. [d] Reference 24. [e] Reference 18. [f] Reference 19. [g] Estimated from refs 18 and 19. [h] Radius of the equivalent sphere calculated from ref 19.

to be pure hydrocarbon with conductivity $\kappa_p = 0$ and permittivity $\epsilon_p = 2$. For its radius R the equivalent sphere radius of the water-free core as determined by SANS is inserted.[19] For the properties of the medium, the same assumptions are made as for Grosse's model. The shell is assumed to consist of the charged headgroups, hydration water, and the Stern layer of adsorbed counterions. Additionally, as suggested by the "hydrophobic hydration numbers" discussed, in part 1, parts of the hydrocarbon tails of the cations may contribute. For the permittivity of this shell, ϵ_s, data estimated by Drummond et al.[24] from the solvatochromism of a series of surface-active acid−base indicators are inserted. However, model calculations show that the results are almost independent of the employed ϵ_s. Simultaneously fitted quantities are S_2 and τ_2, both unweighted. Adjustable parameters of the model are the conductivity, κ_s, and the thickness, d, of the shell.

As can be seen from Figure 6, the model of Pauly and Schwan yields a good fit of the dispersion amplitude S_2 even for the highest examined concentrations.[26] On the other hand, there are slightly larger deviations in the relaxation time τ_2 at low concentrations. The parameter d, listed in Table 3, is of reasonable magnitude and not too different from the values determined by SANS. However, as can be seen from Figure 5, the volume fractions deduced from $R_m = R + d$ are systematically smaller than those obtained with Grosse's model and from the concentration of free water. The conductivity of the shell, κ_s, considerably exceeds the macroscopic dc conductivity of the solution, $\kappa_m \leq 3.7$ S m^{-1} (see the Supporting Information of part 1). Assuming that the relation between conductivity and the ionic diffusion coefficients valid for ordinary electrolyte solutions[13] also applies for the diffusion of the adsorbed halide ions in the conducting shell, one may write for the diffusion coefficient of the bound anions

$$D^S(X^-) = \frac{k_B T \kappa_s}{e_0(1-\alpha)N} \cdot \frac{4\pi}{3}[(R+d)^3 - R^3] \qquad (11)$$

where e_0 is the elementary charge. The results are included in Table 3. The required data for the degree of counterion association, $1 - \alpha$, and the aggregation number of the micelles, N, summarized in Table 2, are taken from the literature. κ_s and thus $D^S(X^-)$ exhibit a similar dependence on the chain length of the surfactant ion and on the counterion as the surface conductivity, λ_s, determined with the help of Grosse's theory. Obviously, both models support the classical picture of the

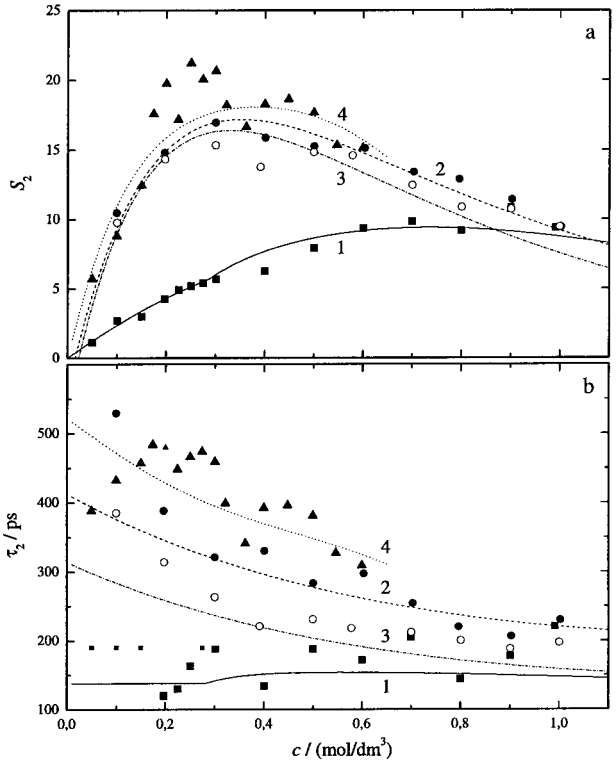

Figure 6. Fit curves obtained with the theory of Pauly and Schwan (lines) and experimental dispersion amplitudes, S_2 (a), and relaxation times, τ_2 (b), of the fast micelle relaxation of C_8TAB (1, ■), C_{12}TAB (2, ●), C_{12}TAC (3, ○), and C_{16}TAB (4, ▲). The model for C_8TAB incorporates the contribution from ion-pair relaxation, see text. Small symbols indicate relaxation parameters which were preset in the analysis of $\hat{\epsilon}(\upsilon)$ and thus not used for the test of the theory.

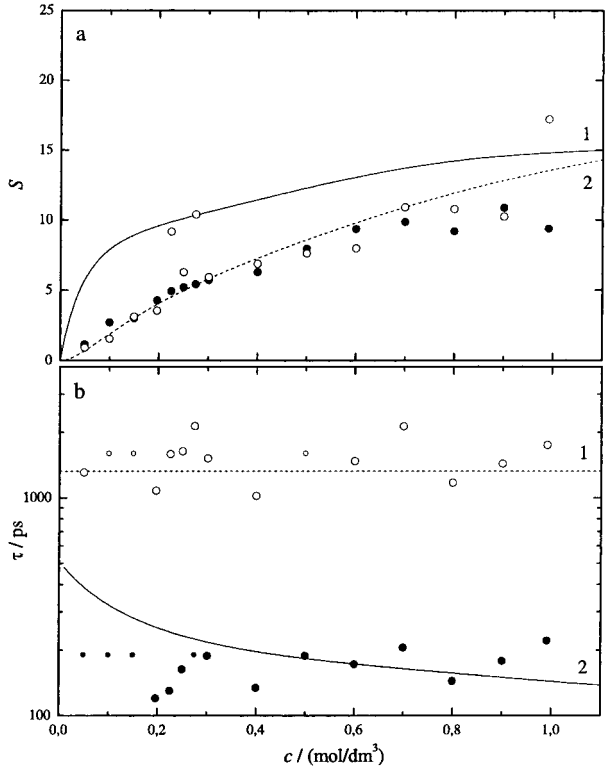

Figure 7. (a) Experimental dispersion amplitudes, S_i, and (b) relaxation times, τ_i, of the micelle relaxation processes $i = 1$ (○) and $i = 2$ (●) of C_8TAB at 25 °C. The lines give the fit of Grosse's model to the low-frequency process, $i = 1$ (broken), and the resulting prediction for $i = 2$ (solid). Small symbols indicate relaxation parameters that were preset in the analysis of $\hat{\epsilon}(\upsilon)$ and thus not used for the test of the theory. For the fit cmc = 0 is assumed, see text.

micelle as an oil droplet with a charged surface, surrounded by a highly conductive layer of condensed (i.e. associated) counterions. Additionally, Grosse's theory treats the diffuse counterion cloud building up around these entities due to elementary electrostatics. Compared to the diffusion coefficients $D^\infty(Cl^-) = 2.032 \times 10^{-9}$ m^2 s^{-1} and $D^\infty(Br^-) = 2.080 \times 10^{-9}$ m^2 s^{-1} of infinitely dilute solutions in water,[21] the mobility of the condensed halide ions is considerably reduced. Interestingly, the difference between chloride and bromide is more pronounced for the micelles. A direct comparison of $D^S(X^-)$ with the literature is only possible for C_{16}TAB. Here Hedin and Furó obtained values ranging from 0.81×10^{-9} to 1.85×10^{-9} m^{2}s^{-1} depending on the applied assumptions.[23] This agrees reasonably with the result of Table 3. When starting the investigation, we expected to see an effect of the well-known sphere-to-rod transition of C_{16}TAB micelles at $c \approx 0.3$ mol/dm^3.[25] Obviously, the transition does not affect the micelle relaxation behavior to a detectable extent. In our opinion this supports the interpretation of the τ_2-relaxation process as a hopping of bound halide ions between adjacent sites on the micelle, governed by the enthalpy of activation, $\Delta H^\ddagger(\tau_2)$, Table 1. Such a nearest-neighbor hopping should be rather independent of the shape of the micelle but depend on the number of available free sites—hence $(1 - \alpha)$—and on the interaction strength between X^- and the polar headgroup of a surfactant ion. On the other hand, according to eq 2 it must be expected that the ion-cloud relaxation depends on the shape of the micelle, because the effective radius should change considerably at the sphere-to-rod transition. However, our data of τ_1 and S_1 are not sufficiently accurate to detect this. More precise information at low frequencies is required to pursue this question.

Octyltrimethylammonium Bromide. As discussed in part 1 the spectra of C_8TAB have to be described by a sum of five Debye equations even at $c <$ cmc. While the parameters S_1 and τ_1 of the octyl salt vary similar to those of the longer chain surfactants, there is a significant difference in the concentration dependence of S_2 and τ_2; see Figure 7. This prevents a simultaneous fit of all four parameters with Grosse's model. But quite surprisingly, with the assumption of cmc = 0 this model yields a good fit of S_1 and τ_1 over the entire concentration range. The deduced results for the radius, R, and the surface conductivity, λ_s, are reasonable and R compares well with the SANS result; see Table 2. This possibly suggests that loose aggregates are formed, which in most aspects differ from a typical micelle, but which are already surrounded by a diffuse ion cloud big enough to produce a detectable dielectric signal. Note that for solutions of conventional electrolytes, like NaCl or tetrabutylammonium bromide, the contribution of the ion-cloud relaxation is too small to be detected.[14,15] In its own, neither the model of Grosse nor the theory of Pauly and Schwan is sufficient to fit $S_2(c)$ and $\tau_2(c)$. However, it is well-known that aqueous solutions of symmetrical tetraalkylammonium halide solutions, including tetramethylammonium bromide, show considerable association to ion pairs.[27,28] These produce a notable dielectric dispersion step with a relaxation time in the same order of magnitude as τ_2.[20,29] Thus, it is reasonable to assume an ion-pair contribution to the dielectric spectra of C_8-TAB, namely to τ_2 and S_2, and at $c <$ cmc the tumbling motion of this species should be the predominating solute relaxation process.

Generally, the dielectric data are used to identify the relaxing ion-pair species as, in contrast to vibrational or NMR spectros-

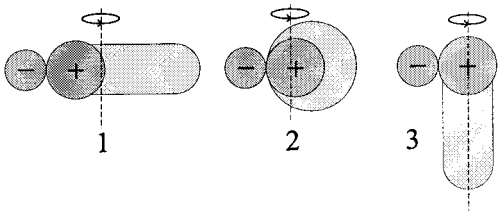

Figure 8. Models for the contact ion pairs considered in the analysis of the C_8TAB: CIP with "stretched" (1), "curled up" (2), and "side-on" (3) surfactant cations. For details see text.

copy, dielectric spectroscopy is sensitive not only to contact ion pairs (CIP) but also to solvent-shared (SSIP) and doubly solvent−solvent-separated (2SIP) ion pairs.[30−32] Ideally, this is done by comparing the equilibrium constant of ion association, K_a, determined from the ion-pair dispersion amplitude for appropriate models of conceivable ion-pair species, with model-independent K_a values from thermodynamic or conductivity measurements (which in itself do not give structural information). The result can be cross-checked by comparing the experimental ion-pair relaxation time, τ_{IP}, with the rotational correlation times, τ', calculated from the size and shape of the considered model ion pairs. Additionally, information on the kinetics of ion-pair formation may be inferred from the typical decrease of $\tau_{IP}(c)$ when the lifetime and the tumbling motion occur on the same time scale.[33] No independent information is available on the structure of possible C_8TAB ion pairs. For the analysis of S_2 and τ_2 of C_8TAB at $c <$ cmc we thus approximate the surfactant cation as a charged headgroup of the radius $r_h = 0.280$ nm of a tetramethylammonium ion[34] plus a hydrocarbon chain of length $l_8 \approx 1.19$ nm (estimated from bond lengths and angles). We consider CIP, where Br^- ($r_- = 0.196$ nm[34]) is in direct contact with the headgroup of the cation, as well as species where the charges are separated by one (SSIP) or two (2SIP) hydration shells of thickness $2r_w = 0.285$ nm.[35] Additionally, one may imagine different ways of folding for the alkyl chain of the surfactant ion in aqueous solution. We consider the three limiting structures shown in Figure 8 for CIP as an example. Model 1 assumes an overall rotation of the ion pair around an axis perpendicular to the fully stretched octyl chain. The length of the chain is estimated from bond distances and angles. Thus, the semiprincipal axes of the ellipsoid representing the ion pair are $a = r_- + nr_w + r_h/2 + l_8/2$ and $b = r_h$. Model 2 is similar but with the alkyl chain completely folded around the ionic headgroup. The cation, including its octyl chain is mimicked by a sphere of radius $r_+ = 0.433$ nm. r_+ is calculated from the partial molar volume of monomeric C_8TAB[36] corrected for the volume of Br^-. The semiprincipal axes for model 2 are $a = r_- + nr_w + r_+$ and $b = r_+$. This is the most probable configuration of the ion pair in aqueous solution as NMR results for $c <$ cmc suggest a strongly folded alkyl chain.[37−40] Model 3 assumes rotation of the ionic headgroup and the associated counterion around the axis determined by the stretched octyl chain. The chain was assumed to be "fixed" in the solution so that the relevant volume of rotation of the ion pair is solely determined by the headgroup and counterion as $a = 2r_- + 2nr_w + r_h$, $b = r_h$. Obviously, this is the most probable configuration for a rotating ion-pair incorporated into the micelle, which was suggested by Shikata and Imai[12] as the possible origin of the τ_2 relaxation process. For the calculation of ion-pair concentrations, c_{IP}, from S_2 and for the estimation of the rotational correlation times, τ', we use the approach described in ref 30. K_a is obtained from c_{IP} as described in ref 32.

The association constants and rotational correlation times of all nine model species are summarized in Table 4. To our knowledge K_a has not been determined by other experimental methods for C_8TAB, This prevents a direct comparison, and thus a clear-cut identification of the species is not possible. However, K_a should be similar to values found for symmetrical tetraalkylammonium bromides, where data range from $K_a = 1.49$ dm^3 mol^{-1} for the methyl compound[41] to $K_a = 7.4$ dm^3 mol^{-1} for the *n*-pentyl salt.[42] Additionally, for C_8TAB micelles the degree of counterion dissociation, $\alpha = 0.35$,[18] is rather large, although one may reasonably assume that the larger charge density on the surface of the micelles should lead to an increased halide binding compared to the surfactant monomer. Thus, the values of $K_a > 100$ required to explain the observed S_2 allow us to rule out contact ion pairs of any of the three models of Figure 8. This is in line with the NMR results of refs.[37,43] The large solvation numbers, Z_{ib}, inferred in part 1 for the headgroups of all investigated surfactant ions also favor SSIP and/or 2SIP.

TABLE 4: Association Constants, K_a, Calculated from S_2, and Rotational Correlation Times, τ', Obtained for Various Ion Pair Geometries of C_8TAB at 25 °C[a]

	model	CIP	SSIP	2SIP
K_a	1	$(3 \pm 2) \times 10^3$	35 ± 9	14 ± 3
	2	$(4 \pm 1) \times 10^2$	26 ± 6	11 ± 3
	3	$(1.1 \pm 0.3) \times 10^2$	21 ± 5	10 ± 2
τ'	1	253	396	581
	2	37	99	195
	3	3	64	232

[a] Units: K_a in dm^3/mol, τ' in 10^{-12} s.

For the limited number of free-running fits of $\hat{\epsilon}(\upsilon)$ the ion-pair relaxation time can be averaged to $\bar{\tau}_2 = 138$ ps within experimental accuracy. This indicates that the ion-pair kinetics is rather slow and it is reasonable to assume that the C_8TAB ion pair has a lifetime similar to that of $(CH_3)_4NBr$, approximately 1 ns.[20] Therefore, $\bar{\tau}_2$ can be directly compared with τ' of Table 4. Obviously, the "streched" ion pair, model 1, can be ruled out in all its variants: CIP, SSIP, and 2SIP. But also the contact ion pairs of the models 2 and 3 are very unlikely, corroborating thus the inference from K_a. The best agreement between $\bar{\tau}_2$ and τ' is found for the SSIP of model 2, that is the ion pair with the folded *n*-octyl chain. Note that SSIP are also observed for tetramethylammonium bromide,[20] where the cation is a good model for the polar headgroup of the surfactant ion. The folded alkyl chain characteristic for model 2 is evidenced by NMR.[37−39]

From the preceding discussion we may conclude that the "free" ion pairs detected for C_8TAB at $c <$ cmc are likely of the solvent-shared type (SSIP) with minimized hydrocarbon−water interactions (model 2). For the equilibrium constant of this species we may estimate $K_a \approx 26$ dm^3 mol^{-1}. Such ion pairs, as well as free ions, are also present at $c >$ cmc and must be considered in the analysis of S_2 and τ_2 with the help of the theory of Pauly and Schwan (Grosse's model is not compatible with cmc ≈ 0.3 mol dm^{-3}). Thus, the dispersion amplitude S_2 is the sum of the ion-pair contribution, S_{ip}, and of the micelle contribution, S_{mic}, where

$$S_{ip}(c) = \begin{cases} S_2(c) & c \le \text{cmc} \\ S_2(\text{cmc}) \cdot (1-p) & c > \text{cmc} \end{cases} \qquad (12)$$

It may be reasonably assumed that in the bulk solution $c_{ip} = c_{ip}(\text{cmc})$ for $c \ge$ cmc so that the amplitude of the ion pair relaxation process decreases linearly with the volume fraction $(1 - p)$ of the bulk solution. For the relaxation time τ_2 a logarithmic average of the two contributions, τ_{ip} and τ_{mic}, weighted by their dispersion amplitudes, was assumed

$$\ln(\tau_2) = \frac{S_{ip}\ln(\tau_{ip}) + S_{mic}\ln(\tau_{mic})}{S_{ip} + S_{mic}} \quad (13)$$

For the ion-pair relaxation time $\bar{\tau}_{ip} = 138$ ps was inserted. In the iteration procedure the data obtained for S_{mic} and τ_{mic} with the model of Pauly and Schwan, eqs 6−9, were used as the input for eqs 12, 13. The fit curves for S_2 and τ_2 obtained for the C_8TAB solutions from the combination of ion-pair relaxation and the model of Pauly and Schwan are included in Figure 6. In view of the necessary assumptions the agreement with the experimental data, especially with S_2, is very satisfactory. Even more pleasing is the fact that the deduced fit parameters, thickness of the conductive shell, $d = 0.76$ nm, and its conductivity, $\kappa_s = 5.7$ S m^{-1}, compare well with the data of the other investigated surfactants; see Table 3. Note that from all the species considered in Table 4 this coherence of results between C_8TAB and the other investigated surfactants is only obtained for the SSIP/model2 ion-pair.

4. Conclusions

The dielectric relaxation behavior of aqueous octyl-, dodecyl-, and hexadecyltrimethylammonium bromide and of dodecyltrimethylammonium chloride solutions exhibits five dispersion steps. Within experimental accuracy, each of them can be modeled by a Debye equation. As discussed in part 1 of this contribution, the high-frequency processes with relaxation times $\tau_3 \approx 25$ ps, $\tau_3 \approx 8$ ps, and $\tau_3 \approx 1$ ps are characteristic for the water and allow inference on micelle hydration. In the present paper it was shown that for C_{12}TAB, C_{12}TAC, and C_{16}TAB the dispersion steps with the relaxation times $\tau_1 \approx 1.5$ ns and $\tau_2 \approx 300$ ps can be assigned to relaxation modes of the micelles. For C_8TAB an additional contribution to the amplitude S_2 possibly arises from the tumbling motion of solvent-shared ion pairs formed by Br^- and hydrated octyltrimethylammonium ions with "curled up" alkyl chain. At low concentrations of C_{12}TAB, C_{12}TAC, and C_{16}TAB, $c \lesssim 0.5$ mol dm^{-3}, Grosse's theory, which predicts a low-frequency relaxation arising from the fluctuations of the diffuse ion cloud surrounding the micelle and a faster mode characteristic for the mobility of the ions bound to the surface of the micelle, simultaneously fits amplitudes and relaxation times of both micelle dispersion steps. S_2 and τ_2 can be fitted over the entire concentration range with the model of Pauly and Schwan, which also determines the mobility of the bound counterions. The volume fractions of the micelles deduced from both theories not only compare well with SANS data from the literature, but are also in good agreement with the values obtained from the analysis of the water relaxation processes. Thus, the proposed analysis of the investigated complex permittivity spectra is self-consistent.

Two mechanisms may be envisaged for the mobility of the bound counterions. One is the hopping of the halide ion between different surfactant headgroups on the surface of the micelles. The second, proposed by Shikata and Imai,[12] is the rotation of ion pairs that are incorporated into the micelles with the stretched alkyl chain of the cation (model 3 of Figure 8). In part 1 it was shown that the charged headgroups of the surfactant ions are strongly hydrated, with hydration numbers $Z_{ib}(0)$ ranging from 7 for C_8TAB to 15 for C_{16}TAB. Additionally, the free ion pairs of C_8TAB are SSIP. CIP can be clearly ruled out. Thus, it is likely that also for the micelles the halide ions are bound to hydrated headgroups. This results in a center-to-center distance of 0.8 nm between the charges of cation and anion in the pair. From the aggregation numbers and the radii of the investigated micelles an average distance between the headgroups of about 1 nm may be estimated. Thus, ion-pair rotation in the conventional sense, that is within the field of a homogeneous frictional force, is difficult to envisage. Additionally, to explain the observed amplitude S_2, a strong increase of the degree of counterion dissociation would be required. This is not supported by literature data. Note that NMR studies are also inconsistent with well-defined ion pairs sitting in the micelle.[23]

Interestingly, for octyltrimethylammonium bromide the low-frequency relaxation attributed to the fluctuations of the diffuse ion cloud is also detectable at $c <$ cmc. On the other hand, no classical micelles are formed in this region and the parameters of the second process, S_2 and τ_2, can be reasonably explained by the tumbling motion of SSIP. This suggests that at low concentrations the surfactant ions, free as well as in ion pairs, form loose aggregates surrounded by a sufficiently large cloud of counterions to produce S_1. Hints at such premicellar aggregation also come from light scattering,[18] ^{1}H NMR chemical shifts,[37] and studies of the reaction kinetics in (sub)micellar solutions.[44] Further dielectric investigations into this subject are currently undertaken.

Acknowledgment. We thank Prof. emeritus J. Barthel for encouragement and continuous interest in our work. Financial support by the Deutsche Forschungsgemeinschaft and the Fonds der Chemischen Industrie is gratefully acknowledged.

References and Notes

(1) Evans, D. F.; Wennerström, H. *The Colloidal Domain*, 2nd ed.; Wiley-VCH: New York, 1999.
(2) Lindman, B.; Wennerström, H. *Top. Curr. Chem.* **1980**, *87*, 1.
(3) Barchini, R.; Pottel, R. *J. Phys. Chem.* **1994**, *98*, 7899.
(4) O'Konski, C. T. *J. Phys. Chem.* **1960**, *64*, 605.
(5) Schwarz, G. *J. Phys. Chem.* **1962**, *66*, 2636.
(6) Pauly, H.; Schwan, H. P. *Z. Naturforsch. B* **1959**, *14*, 125.
(7) Schurr, J. M. *J. Phys. Chem.* **1964**, *68*, 2407.
(8) Grosse, C. *J. Phys. Chem.* **1988**, *92*, 3905.
(9) Cavell, E. A. S. *J. Colloid Interface Sci.* **1977**, *62*, 495.
(10) Cavell, E. A. *S. J. Chem. Soc., Faraday Trans. 2* **1984**, *80*, 447.
(11) Falkenhagen, H. *Theorie der Elektrolyte*; S. Hirzel: Leipzig, 1971.
(12) Shikata, T.; Imai, S. *Langmuir* **1998**, *14*, 6804.
(13) Bockris, J. O'M.; Reddy, A. K. N. *Modern Electrochemistry 1. Ionics*, 2nd ed.; Plenum Press: New York, 1998.
(14) Turq, P.; Barthel, J.; Chemla, M. *Transport, Relaxation and Kinetic Processes in Electrolyte Solutions*; Springer: Berlin, 1992.
(15) Barthel, J.; Krienke, H.; Kunz, W. *Physical Chemistry of Electrolyte Solutions*; Steinkopff: Darmstadt and Springer: New York, 1998.
(16) Mukerjee, P. *Adv. Colloid Interface Sci.* **1967**, *1*, 241.
(17) Baar, C.; Buchner, R.; Kunz, W. *J. Phys. Chem. B* **2001**, *105*, 2906.
(18) Drifford, M.; Belloni, L.; Dubois, M. *J. Colloid Interface Sci.* **1987**, *118*, 50.
(19) Berr, S.; Jones, R. R. M.; Johnson, J. S. *J. Phys. Chem.* **1992**, *96*, 5611.
(20) Buchner, R.; Barthel, J.; Hölzl, C.; Stauber, J. Manuscript in preparation.
(21) Lide, D. R. Ed. *CRC Handbook of Chemistry and Physics*, 76th ed.; CRC Press: Boca Raton, New York, London, Tokyo, 1995.
(22) (a) Gaillon, L.; Hamidi, M.; Lelièvre, J.; Gaboriaud, R. *J. Chim. Phys.* **1997**, *94*, 707. (b) Gaillon, L.; Gaboriaud, R. *J. Chim. Phys.* **1997**, *94*, 728.
(23) Hedin, N.; Furó, I. *J. Phys. Chem. B* **1999**, *103*, 9640.
(24) Drummond, C. J.; Grieser, F.; Healy, T. W. *J. Phys. Chem.* **1988**, *92*, 2604.
(25) Backlund, S.; Høiland, H.; Kvammen, O. J.; Ljosland, E. *Acta Chem. Scand. A* **1982**, *36*, 698.
(26) Due to its small amplitude the dispersion step of "slow water", S_3, cannot be resolved for C_{16}TAB at $c \leq 0.15$ mol/L and it is very sensitive to experimental noise at $0.17 \leq c/(\text{mol/L}) \leq 0.27$. Thus, in contrast to the other samples, the amplitude S_2 of C_{16}TAB is systematically biased at $c \leq 0.27$ mol/L and would have justified neglection of the data. However, the corresponding relaxation time decreases smoothly with concentration; i.e., τ_2 is not affected within experimental accuracy. Comparison of the results with and without inclusion of the problematic data shows that the parameters κ_s and d, which are obtained from simultaneously fitting S_2(C) and τ_2(C), differ by less than 15%. Since random scatter on the order of 10% is obvious

for S_2 and τ_2 over the entire concentration range, we prefer to show the "unpolished" results for C_{16}TAB in Figure 6.

(27) Levien, B. J. *Aust. J. Chem.* **1965**, *18*, 1161.
(28) Wirth, H. E. *J. Phys. Chem.* **1967**, *71*, 2922.
(29) Pottel, R.; Lossen, O. *Ber. Bunsen-Ges. Phys. Chem.* **1967**, *71*, 135.
(30) Barthel, J.; Hetzenauer, H.; Buchner, R. *Ber. Bunsen-Ges. Phys. Chem.* **1992**, *96*, 1424.
(31) Barthel, J.; Buchner, R.; Eberspächer, P.-N.; Münsterer, M.; Stauber, J.; Wurm, B. *J. Mol. Liq.* **1998**, *78*, 83.
(32) Buchner, R.; Capewell, S. G.; Hefter, G. T.; May, P. M. *J. Phys. Chem. B* **1999**, *103*, 1185.
(33) Buchner, R.; Barthel, J. *J. Mol. Liq.* **1995**, *63*, 55.
(34) Marcus, Y.; Hefter, G.; Pang, T.-S. *J. Chem. Soc., Faraday Trans.* **1994**, *90*, 1899.
(35) Gibbs, J. H.; Cohen, C.; Fleming, P. D.; Porosoff, H. In *The Physical Chemistry of Aqueous Systems*; Kay, R. L., Ed.; Plenum: New York, 1973.
(36) Tanaka, M.; Kaneshina, S.; Nishimoto, W.; Takabatake, H. *Bull. Chem. Soc. Jpn.* **1973**, *46*, 364.
(37) Bacaloglu, R.; Bunton, C. A.; Cerichelli, G.; Ortega, F. *J. Phys. Chem.* **1989**, *93*, 1490.
(38) Bacaloglu, R.; Blaskó, A.; Bunton, C. A.; Cerichelli, G.; Shirazi, A. *Langmuir* **1991**, *7*, 1107.
(39) Bazito, R. C.; El Seoud, O. A.; Barlow, G. K.; Halstead, T. K. *Ber. Bunsen-Ges. Phys. Chem.* **1997**, *101*, 1933.
(40) Marcus, Y. *Ion Solvation*; Wiley and Sons Ltd.: Chichester, U.K., 1985.
(41) Levien, B. J. *Aust. J. Chem.* **1965**, *18*, 1161.
(42) Kay, R. L.; Evans, D. F.; Cunningham, G. P. *J. Phys. Chem.* **1969**, *73*, 3322.
(43) Lindblom, G.; Lindman, B. *J. Phys. Chem.* **1973**, *77*, 2531.
(44) Bacaloglu, R.; Bunton, C. A. *J. Colloid Interface Sci.* **1987**, *115*, 288.